Biomed Microdevices (2006) 8:353–359
DOI 10.1007/s10544-006-9818-4

2-dimensional MEMS dielectrophoresis device for osteoblast cell stimulation

H. Zou · S. Mellon · R. R. A. Syms · K. E. Tanner

Published online: 14 August 2006
© Springer Science + Business Media, LLC 2006

Abstract A fixed microelectrode device for cell stimulation has been designed and fabricated using micro-electro-mechanical systems (MEMS) technology. Dielectrophoretic forces obtained from non-uniform electric fields were used for manipulating and positioning osteoblasts. The experiments show that the osteoblasts experience positive dielectrophoresis (p-DEP) when suspended in iso-osmotic culture medium and exposed to AC fields at 5 MHz frequency. Negative dielectrophoresis (n-DEP) is obtained at 0.1 MHz. The viability of osteoblasts under dielectrophoresis has been investigated. The viability values for cells exposed to DEP are nearly three times higher than the control values, indicating that dielectrophoresis may have an anabolic effect on osteoblasts.

Keywords Micro-electro-mechanical systems · Dielectrophoresis · Osteoblasts

1 Introduction

Osteoblasts are one of the three major cell types found in bone. Their role is to build and maintain the bony skeleton (Calvi et al., 2003; Gong, 1978; Lord et al., 1975; Taichman and Emerson, 1994; Taichman et al., 1996; Taichman et al., 2001). It has been known since the 19th century that mechanical loading affects the architecture of the musculoskeletal system and this is known as "Wolff's Law". The homeostatic balance that exists in bone between resorption and deposition can be shifted depending on the loading the bone experiences. Reduced loading as a result of extended bed rest or space flight will decrease bone density through increased resorption relative to bone deposition. Conversely increased dynamic loading of bone, in activities such as weightlifting or racquet sports, increases bone density (Turner, 1998). Bone cells are believed to process loading information because bone tissue is poorly innervated and thus does not rely on the central nervous system to integrate and distribute information about mechanical signals (Schrifer et al., 2005). The exact pathways bone cells employ to do this are unknown despite many *in vivo* and *in vitro* studies. In the last decade a range of laboratory apparatuses have been devised and employed to stimulate cells and tissue cultures mechanically (Brown, 2000). The main classes of *in vitro* models generate fluid shear, hydrostatic compression, biaxial stretch, uniaxial stretch or some combination of two or more of these. However, all these have loaded the cells by deforming the substrate to which the cells have attached, or the fluid in which they are cultured.

The aim of this study is to establish a micro-electro-mechanical system (MEMS) platform to study the osteoblast cellular response to local electrical, mechanical, topographic and biochemical cues. A primary challenge in constructing cell-based devices is isolation and precise positioning of a controlled number of osteoblasts on a microdevice. Cell positioning by dielectrophoresis is probably the most broadly applied method among all chip-based cell separation technologies (Führ and Wangner, 1994; Führ and Shirley, 1995, 1998; Lee and Tai, 1999; Jones and Kallio, 1979; Pohl and Pollack, 1979a, 1979b; Pohl et al., 1984; Porschke, 1985; Sato et al., 1990; Washizu, 1990; Wilkinson, 1998; Zimmermann, 1982a; Zimmermann and Pilwat, 1982b).

H. Zou (✉) · R. R. A. Syms
Optical and Semiconductor Devices Group, EEE Dept., Imperial College, Exhibition Road, London, SW7 2AZ, UK
e-mail: h.zou@imperial.ac.uk

S. Mellon · K. E. Tanner
Department of Materials, Queen Mary University, Mile End Road, London, E1 4NS, UK

However, little has been reported on osteoblast stimulation by dielectrophoretic manipulation (Chehroudi et al., 1997; Scotchford et al., 1998; Yang et al., 2003).

The present study has investigated the range of effects of dielectrophoresis on osteoblasts. The initial work involves the design and fabrication of MEMS components. The application of forces to individual cells involves osteoblast preparation and management, and investigative experiments based on microscopy and biochemical analysis. This work is ultimately directed at investigating the mechanisms underlying Wolff's law of bone growth dynamics at the cellular level (Rubin, 1984). The intension is that the methods used can be developed further to control osteoblast metabolism and enhance bone repair processes.

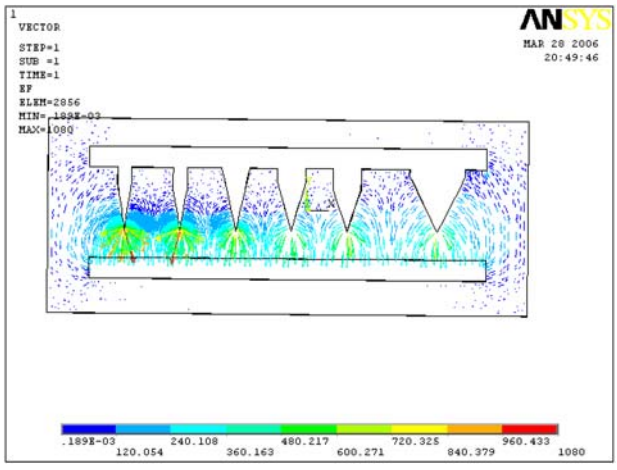

Fig. 1 Electrical field created by sawtooth electrodes with different tip angles (16.26°, 18.92°, 25.06°, 31.89°, 36.87° and 53.13°). The gap between the tips and the bar electrode was held at 10 μm and between the tips was 20 μm (except between 36.87° and 53.13° which was 40 μm)

2 Material and methods

2.1 Modelling and calculations

Dielectrophoresis is defined as the force caused by polarization effects in a non-uniform electric field. Extending this physical concept to a small spherical particle in a medium in a region of non-uniform electric fields, the DEP force on the particle is shown to be (Pethig, 1996)

$$F_{DEP} = 2\pi\varepsilon_l R^3 R_e[f_{CM}]\nabla E_{rms}^2 \tag{1}$$

where, ε_l is the permittivity of the surrounding liquid medium, R is the radius of the particle, E_{rms} represents the root mean square of the electric field experienced by the particle. $R_e[f_{CM}]$ is the real part of the Clausius-Mosotti (CM) factor, which for a homogenous particle is given by:

$$R_e[f_{CM}] = R_e[(\varepsilon_p - \varepsilon_l)/(\varepsilon_p + 2\varepsilon_l)] \tag{2}$$

where, ε_p is the permittivity of the particle and ε_l the permittivity of the liquid medium. ε_x is the complex permittivity for either l or p, and is given by:

$$\varepsilon_x = \varepsilon_x' - j(\sigma_x/2\pi f) \tag{3}$$

where ε_x' is the real part of the complex permittivity, σ_x is the conductivity and f is the frequency.

The particle undergoes positive DEP if $\varepsilon_{p>}\varepsilon_l$ and thus the associated term $R_e[f_{CM}]$ is positive. The neutral particle is then attracted to the region of high field intensity. Conversely the particle undergoes negative DEP if the CM factor is negative ($\varepsilon_{p<}\varepsilon_l$) and the DEP force will repel the particle towards regions of lower field strength.

In this work, microelectrodes were used to create the non-uniform field necessary to generate dielectrophoretic forces. The electrodes were designed in interdigitated arrays with

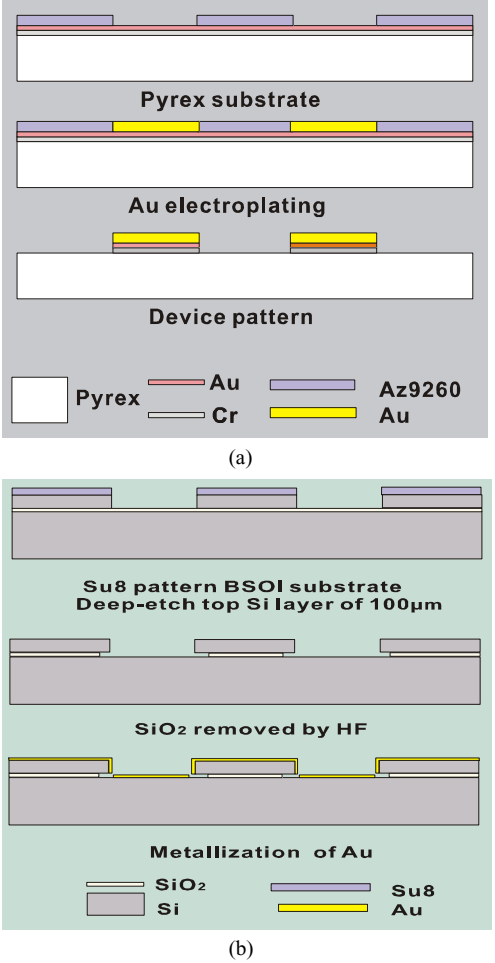

Fig. 2 Schematic diagram of the device fabrication using: (a) Pyrex substrate and (b) BSOI substrate

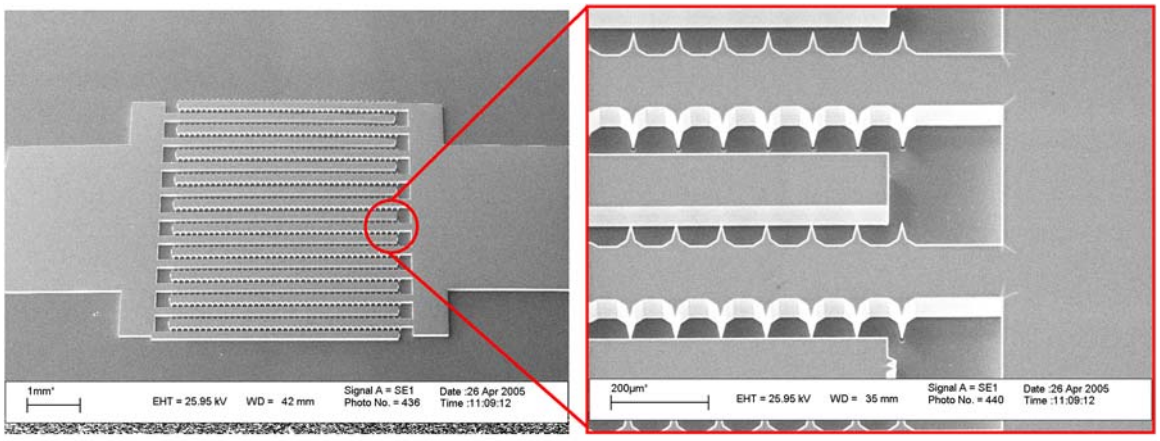

Fig. 3 Scanning electron microscope photographs of a complete device on BSOI substrate. (a) the overall layout of a device (marker bar = 1 mm), (b) a close-up of the interdigitated arrays (marker bar = 200 μm)

triangle and bar tooth profiles. The maximum electric field occurs in the region of any sharp tips. A range of gaps between opposing electrodes were designed to vary from 10 μm to 80 μm in order to supply different intensities of electric field. The electric fields were modeled using ANSYS, a finite element software package, to solve the Laplace equation. As the microelectrodes were essentially two-dimensional a two–dimensional model was sufficient to describe the system. For simplicity the device was modeled as if surrounded by air. Figure 1 shows an ANSYS simulation of the electric field distribution created by microelectrodes containing sharp features. It can be seen that the highest electric field occurs in the vicinity of the sharp tips.

2.2 Device fabrication

Two processing techniques were used to prepare devices. The two substrates for the electrodes were Pyrex and bonded silicon on insulator (BSOI). The transparent Pyrex substrates enabled monitoring of cells attached to the device throughout the experiment using transmission optical microscopy.

Figure 2(a) shows the process flow for devices on Pyrex. In brief, chrome (30 nm thick) and copper (200 nm) seed layers were sequentially sputtered onto a 4″ Pyrex glass wafer. Gold (10 μm thick) microelectrodes were deposited inside a photoresist mould by electroplating. The seed layers were then removed by wet etching. Finally, individual test cells were separated using a diamond saw. A total of 68 devices were generated from each wafer.

Devices were also fabricated by deep reactive ion etching (DRIE) of bonded silicon on insulator (BSOI) substrates (Klaassen et al., 1996). Although further electrostatic modeling shows that the use of a conducting substrate shorts out the electric field near the substrate, this effect appears to be outweighed away from the substrate by the field enhancement obtained using the sharper electrode tips that can be achieved by etching.

Figure 2(b) shows the process flow for devices on BSOI. The material was obtained commercially from Analog Devices (Belfast, UK), and consisted of 4″ diameter (100) orientated Si, with a bonded layer thickness of 100 μm and an oxide interlayer thickness of 2 μm. First a dehydration bake of the BSOI wafer was performed in an oven at 150°C for 30 minutes. The device layer side was then patterned using SU8-2000 negative photoresist and deep etched down to the oxide interlayer. Deep etching was performed using a Surface Technology Systems inductively coupled plasma etcher, using a photoresist hard mask and cyclic etching with SF_6 and passivation with C_4F_8 (Hynes et al., 1999) The hard mask was then removed by wet stripping followed by plasma etching in O_2. The sacrificial oxide was then etched from beneath the top silicon layer using buffered hydrofluoric (HF) acid. The wafer was then finally metallized with 30 nm Cr and 300 nm Au by conformal sputtering to provide electrical contacts. Electrical isolation between opposing electrodes is

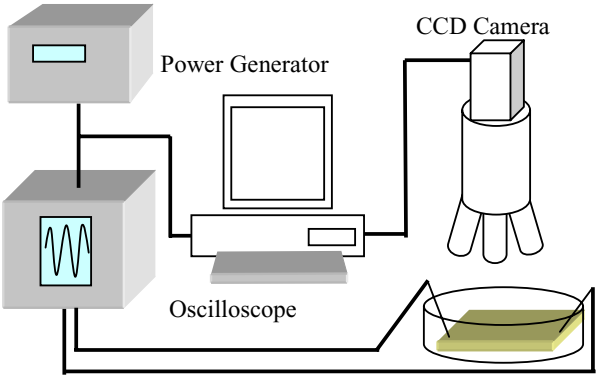

Fig. 4 Schematic view of the experimental set-up showing a signal generator connected through to the device in a Petri dish

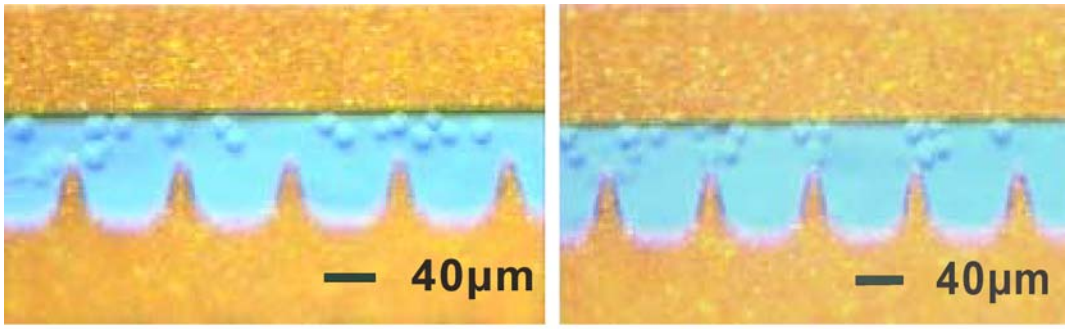

Fig. 5 (a) The osteoblast cells are randomly distributed around the electrodes on Pyrex wafer without AC power; (b) Once AC power was applied, osteoblast cells aggregated around electrode tips by positive DEP (marker bars = 40 μm) on Pyrex wafer device

provided by the large lateral HF undercut, which prevents metal tracking between the interdigitated arrays. Figure 3 shows scanning electron microscope photographs of a complete device on BSOI. Figure 3(a) shows the overall layout of a device, while Fig. 3(b) shows a close-up of the interdigitated arrays

2.3 Cell culture and reagents

HOS TE-85 osteosarcoma cells were grown in culture medium consisting of DMEM (Sigma, UK) supplemented with 10% Fetal Calf Serum (FCS) (First Link Ltd. UK), HEPES buffer, MEM non-essential amino acid, L-glutamine, Penicillin-Streptomycin and Ascorbic acid (all Sigma, UK). The cells were maintained in an incubator at 37°C and 5% CO_2 until required for DEP.

For DEP experiments cells suspended in culture medium were centrifuged for 5 minutes at 2000 rpm, the supernatant was discarded and cells were re-suspended in a 300 mM sucrose solution with 1% FCS. The conductivity of this solution was measured at approximately 10 mS m^{-1} compared to approximately 1.8 S m^{-1} for the culture medium.

2.4 Device operation

The experimental set-up is shown in Fig. 4. The osteoblast cells were immersed in a liquid-filled Petri dish containing culture medium. A sinusoidal voltage was supplied across two bus bars connected to an interdigitated array to produce the non-uniform electric field. The TG1010A signal generator (TTi, Cambridge, UK) produces AC power with frequency in the range of 1 Hz to 10 MHz and voltages of 1 to 20 Vpp. The AC signal was sinusoidal and had a frequency of 5 MHz and for cell stimulation this was pulsed on and off at 1 Hz for 45 min. The resulting cell behavior was monitored via a microscope and camera and recorded on a video file for future analysis. For devices on Pyrex, the Petri dish was placed on an inverted microscope so that the cells could be viewed. For devices on BSOI, the illumination was from above using a standard microscope.

3 Results

3.1 Dielectrophoresis

Figure 5(a) shows that the osteoblast cells are randomly distributed around the electrodes on a Pyrex device prior to applying AC power. AC power at 5 MHz and 10 Vpp caused osteoblast cells to aggregate around the tips of electrodes by positive DEP as shown in Fig. 5(b). Similar effects were caused in BSOI devices, as shown in Fig. 6, However, BSOI devices appeared to produce greater DEP forces due to the sharper electrode tips produced by the deep RIE processing.

Figure 7 shows the effect of negative dielectrophoretic forces on a Pyrex device. The osteoblasts experience negative

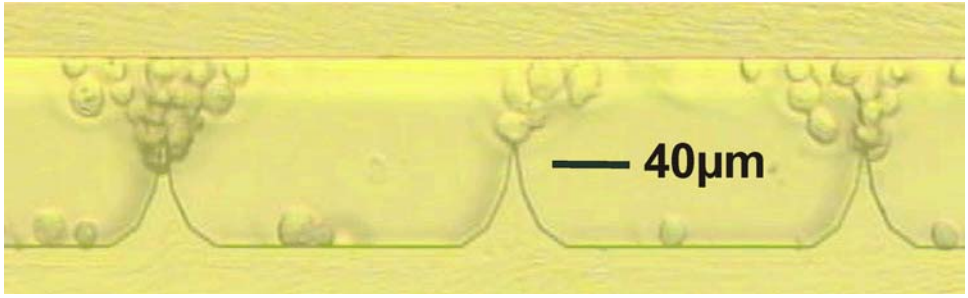

Fig. 6 Once AC power was applied, osteoblast cells aggregated around the tips of electrodes by positive DEP on the BSOI wafer device (marker bar = 40 μm)

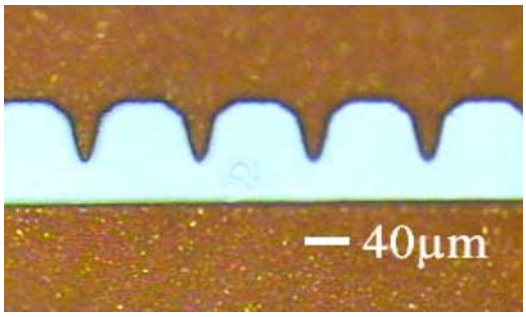

Fig. 7 An osteoblast cell is repelled from electrode tip at 0.1 MHz 20 Vpp by negative DEP (marker bar = 40 μm) on Pyrex wafer device

DEP using electric fields generated at 0.1 MHz, which repels the cell away from the tips of the electrodes.

3.2 Viability test

The effect of dielectrophoretic stimulation on osteoblast viability was investigated. This test utilizes a dye (Alamar blue^{TM}) that fluoresces in response to medium reduction caused as a result of cell metabolism i.e. the action of active mitochondria. The results give an indication of a combination of cell population size and cell metabolism. A large population will result in the activation of more of the fluorescent dye in the medium. Similarly a number of cells with a raised level of metabolism will activate more dye resulting with a higher recorded fluorescence. The cells themselves do not fluoresce but rather the medium in which they grow. The medium is removed, placed in a separate well plate and analyzed spectro-fluorometrically.

Figure 8 shows the schematic diagram of the experimental set-up for the test of osteoblast viability. Twelve separate Pyrex devices were prepared. Cells were exposed to positive DEP forces for 45 minutes on six devices, while another

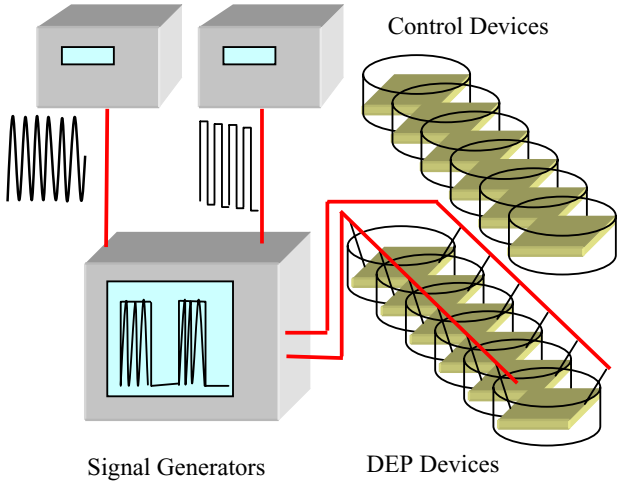

Fig. 8 Schematic diagram of the experimental set-up for the test of osteoblast viability

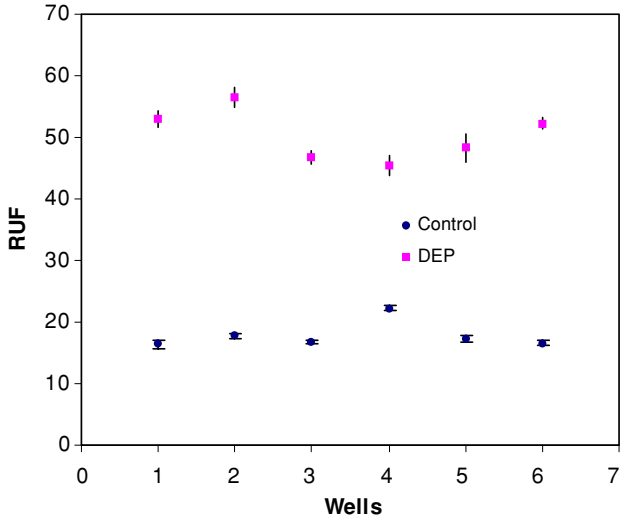

Fig. 9 Scatter graph displaying difference in viability of cells on DEP stimulated (5 MHz, 20 Vpp, tip to bar electrode 40 μm) and non stimulated controls

six devices were used as controls. To ensure that osteoblasts lay in the correct position on the devices, the electrodes in the DEP group were energized during cell seeding. Cells on the non-stimulated control group were allowed to distribute randomly. Immediately after the 45 minutes stimulation a test was conducted, using Alamar blue^{TM} dye, to determine the viability of cells in both the control and the DEP group. The sucrose medium was removed and the cells were washed three times with phosphate buffered saline (PBS). Finally culture medium containing 10% Alamar blue^{TM} dye was added. After incubation for four hours at 37°C and 5% CO_2 this medium was removed and placed in a 96 well plate for analysis using a Fluoroskan Ascent plate reader (Labsystems, Thermo, Basingstoke UK) to measure the fluorescence of the Alamar blue, with 6 repeat measures per device.

Figure 9 and Table 1 show the results of the measurements for relative fluorescence. It can be seen from Table 1 that the DEP fluorescence values of 50.3 (in Relative Units of Fluorescence, RUF) are higher than the control values of 17.8 RUF. The values of blank wells, in which dye was incubated with no cells, recorded an average value of 10.5.

4 Discussion

DEP cell separation has considerable promise for biotechnological applications. There is extensive of published work on the different separation techniques, but less on the effects of these forces on cells. Heida and colleagues (Heida et al., 2002) allowed postnatal rat cortical cells to adhere between electrodes. A sinusoidal signal of 3 Volts at 14 MHz was applied. The viability of the cells and the morphology

Table 1 Relative fluorescence data for comparison of DEP group (5 MHz 20 Vpp and tip to bar electrode distance of 40 μm) and Control group

Device no	1	2	3	4	5	6	Average
Control	17.3	18.3	17.1	21.8	17.6	16.4	
	16.4	17.4	16.3	22.5	16.8	17.3	
	17.3	17.3	16.7	21.7	16.9	16.6	
	15.8	17.3	16.9	22.3	17.2	15.8	
	15.8	18.1	16.9	22.7	18.2	16.8	
	16.1	18.0	17.0	22.4	17.1	16.8	
Average	16.4	17.7	16.8	22.2	17.3	16.6	17.8
ST Dev.	0.69	0.45	0.28	0.39	0.52	0.49	2.08
DEP	55.0	56.0	48.0	42.7	46.1	52.2	
	54.1	55.2	45.7	45.1	52.2	50.3	
	52.6	54.2	45.4	45.2	48.6	53.1	
	52.2	56.8	47.4	47.6	45.6	53.1	
	51.6	57.7	46.8	45.6	47.6	52.7	
	52.6	58.5	47.1	45.8	49.4	52.3	
Average	53.0	56.4	46.7	45.3	48.2	52.2	50.3
ST Dev.	1.27	1.59	1.00	1.59	2.43	1.04	4.18

of exposed cells were similar to non-exposed cells. Archer et al. (1999) used a fibroblastic cell line (BHK 21 C13) which was examined for cell division, morphology, respiration and gene expression in response to a 5 MHz, 21 V electric field applied across a 100 μm gap. Cell morphology, division and respiration were all normal. Proteins associated with heat-shock were up-regulated, although temperature recorded during electric field stimulation and in controls was unchanged throughout the experiment. Wang et al. (1999) conducted a study using a mouse erthroleukemia cell line (DS19) to consider the effects of DEP field exposure on cell proliferation and viability. A 7 V signal was applied in the frequency range 100 Hz–10 MHz using various medium conductivities. Exposure to electrical fields above 10 kHz had no detectable effect on cell growth kinetics for all three conductivities. However field exposure at frequencies below 10 kHz caused a decrease in cell growth. This effect was similar to untreated cells exposed to treated medium. Medium that had undergone field exposure was added to cells that were not exposed to the electrical field. These findings suggested that electrochemical products generated during DEP were responsible for changes in cell growth. Glasser and Führ (1998) used a fibroblastic mouse cell line (L929) exposed to fields to test for cell division and cell viability. They found that cell proliferation ceased after prolonged exposure to trans-membrane potentials of 130–150 mV. However a frequency window was found at frequencies above 1 MHz when strong fields applied were capable of manipulating cell position without any distress to cells.

This work demonstrates the use of dielectrophoretic forces to simultaneously manipulate and position suspended osteoblast cells on microelectrode arrays. The results show

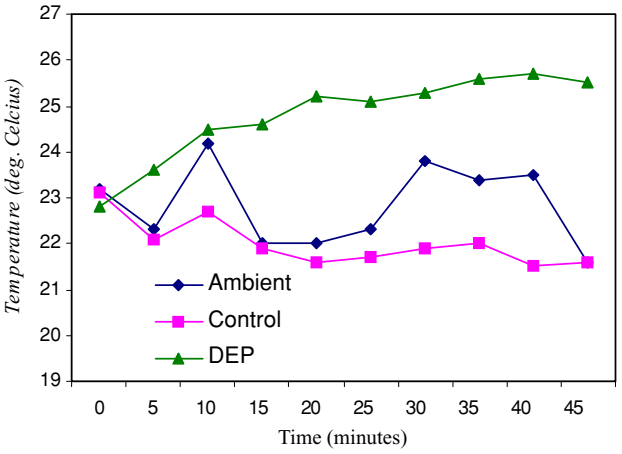

Fig. 10 Temperature (°C) of sucrose solution recorder over 45 mins with (DEP) and without (control) dielectrophoretic stimulation (20 Vpp and 5 MHz)

that the osteoblasts experience p-DEP when suspended in a sucrose solution (at room temperature) and exposed to AC fields at 5 MHz, and n-DEP using 0.1 MHz.

The viability of osteoblasts under dielectrophoresis has also been investigated. The amount of fluorescent dye activated in response to cells stimulated using DEP was greater than the non-stimulated groups. Temperature readings taken during stimulation indicate an increase of approximately 3°C above ambient and control readings (Fig. 10). This difference could be attributed to Joule heating occurring at the electrodes, but considering the experiment was conducted below ideal culturing temperatures (37°C) in a solution lacking vital ingredients this change is insignificant. Electrolysis at the electrodes producing free radicals or a change of pH is another difference to be explored. However, the increased activation of the dye could not be as a result of reactive species in the sucrose solution created by DEP as the devices were thoroughly washed after stimulation to remove the sucrose solution. The cells exposed to DEP may have increased metabolism in response to the loading as a result of DEP forces. Mechanical loading has been shown to have an anabolic effect on bone cells (Rubin, 1984).

Future work will focus device optimization for cell stimulation studies. A future aim is to carry out cyclic stressing over long and short time periods on cells adhered between electrodes. A study of cell morphology using scanning electron microscopy may reveal osteoblast reaction to positive or negative-DEP forces between electrodes. By varying the voltage and/or frequency of the stimulation it may be possible to explore the mechanical-transductive behavior of osteoblast cells.

Acknowledgments The authors wish to thank Dr. J. P. Stagg for assistance with DRIE processing throughout this work. S. Mellon wishes to thank EPSRC (UK) for a studentship.

References

S. Archer, L.A. Tong-Tong, T. Evans, S.T. Britland, and H. Morgan, Biochemical and Biophysical Research Communications **257,** 687 (1999).

T.D. Brown, J. Biomech. **33**, 3 (2000).

L.M. Calvi, G.B. Adams, K.W. Weibrecht, J.M. Weber, D.P. Olson, M.C. Knight, R.P. Martin, E. Schipani, P. Divieti, F.R. Bringhurst, L.A. Milner, H.M. Kronenberg, and D.T. Scadden, Nature **425**, 841 (2003).

B. Chehroudi, D. McDonnel, and D.M. Brunette, J. Biomed. Mater. Res. **34**, 279 (1997).

G. Führ and B. Wagner, Proc. Microsystems '94 Berlin **19–21**, 407 (1994).

G. Führ and S.G. Shirley, J. Micromech. Microeng. **5**, 77 (1995).

G. Führ and S.G. Shirley, Top. Curr. Chem. **194**, 83 (1998).

H. Glasser and G. Fuhr, Bioelectrochemistry and Bioenergetics **47**, 301 (1998).

J.K. Gong, Science **199**, 1443 (1978).

T. Heida, P. Vulto, W.L. Rutten, and E. Marani, Journal of Neuroscience Methods **110**, 37 (2002).

A.M. Hynes, H. Ashraf, J.K. Bhardwaj, J. Hopkins, I. Johnston, and J.M. Shepherd, Sensors Actuators **74**, 13 (1999).

T.B. Jones and G.A. Kallio, J. Electrostat. **6**, 207 (1979).

E.H. Klaassen, K. Petersen, J.M. Noworolski, J. Logan, N.I. Maluf, J. Brown, C. Storment, W. McCulley, and T.A. Kovacs, Sensors Actuators A **52**, 132 (1996).

S.W. Lee and Y.C. Tai, Sensors and Actuators A **73**, 74 (1999).

B.I. Lord, N.G. Testa, and J.H. Hendry, Blood **46**, 65 (1975).

R. Pethig, Critical Review of Biotechnology **16**, 331 (1996).

H. Pohl and K. Pollack, J. Electrostat. **5**, 337 (1979a).

H. Pohl and K. Kaler, Cell Biophys. **1**, 15 (1979b).

H. Pohl, K. Pollock, and H. Rivera, J. Quant. Chem. **11**, 327 (1984).

D. Porschke, Ann. Rev. Phys. Chem. **36**, 159 (1985).

C.T. Rubin, J. Bone Jt. Surg A, **66**, 397 (1984).

K. Sato, Y. Kawamura, S. Tanaka, K. Uchida, and H. Kohida, Sensors and Actuators A, **21–23**, 948 (1990).

J.L. Schriefer, S.J. Warden, L.K. Saxon, A.G. Robling, C.H.Turner, J. Biomech. **38**, 1838 (2005).

C.A. Scotchford, E. Cooper, G.J. Leggett, S. Downes, J. Biomed. Mater. Res. **41**, 117 (1998).

R.S. Taichman and S.G. Emerson, J. Exp. Med. **179**, 1677 (1994).

R.S. Taichman, M.J. Reilly, and S.G. Emerson, Blood **87**, 518 (1996).

R.S. Taichman, M. Reilly, R. Verma, K. Ehrenman, and S. Emerson, Br. J. Haematol **112**, 438 (2001).

C.H. Turner, Bone **23**, 399 (1998).

X. Wang, J. Yang, and P.R. Gascoyne, Biochimica et Biophysica Acta, **1426**, 53 (1999).

M. Washizu, J. Electrostat. **25**, 109 (1990).

C.D.W. Wilkinson, A.S.G. Curtis, and J. Crossan, JVST **B16**, 3132 (1998).

M. Yang, S. Prasad, X. Zhang, A. Morgan, M. Ozkan, and C.S. Ozkan, Sensors and Materials **15**, 313 (2003).

U. Zimmermann, Biochim. Biophys. Acta **694**, 227 (1982a).

U. Zimmermann and G. Pilwat, and H. Pohl, Biol. Phys. **10**, 43 (1982b).